Thermodynamic Properties of Polyaromatic Hydrocarbons Adsorption from Wastewater using Pineapple-Crown-Based Cellulose

Oladimeji, F.O. ^{1,2,3}, Alade, A.O. ^{1,2,3,4}, Tijani, I.O. ^{1,2,3}, Abdulrasheed, W.A. ^{1,2,3}, Olarinde, M.O. ^{1,2,3}, Ilori, K.P. ^{1,2,3}, Agoro, M.K. ^{1,2,3}, Olatunji, A.O. ⁵, Egbeyemi, A.O. ^{1,2,3}, and Afolabi, T.J. ^{1,2,3}

¹ Department of Chemical Engineering, Faculty of Engineering, Ladoke Akintola University of Technology, (LAUTECH), Ogbomoso, Nigeria

² Bioenvironmental, Water and Engineering Research Group (BWERG), LAUTECH, Ogbomoso, Nigeria
 ³ LAUTECH SDG 6 Research Cluster (LSDGRC-6), Ladoke Akintola University of Technology, P.M.B. 4000, Ogbomoso, Nigeria

⁴ Science and Engineering Research Group (SAERG), (LAUTECH), Ogbomoso, Nigeria

Corresponding author. E-mail: aoalade@lautech.edu.ng and +2347037885961

Abstract: The high concentration of Polyaromatic hydrocarbons (PAHs) in produced water which are possibly carcinogenic both to humans and wildlife animals poses a significant threat to the environment giving rise to the need for a sustainable and economical method for PAHs elimination in produced water which is the use of Pineapple crown cellulose (PCC) as an adsorbent in the wastewater treatments as conventional methods are not efficient. The thermodynamic properties of batch adsorption of the PAHs in produced water onto the PCC, under the effect of temperature, were investigated in this study. The raw pineapple crown leaves were processed, treated with NaOH aqueous solution before being washed and dried and then used for the treatment of produced water containing a multi-component mixture of P-Nitrophenol, Naphthalene, Acenaphthene and Pyrene, using batch adsorption method at varying temperatures (40-60 °C). Thermodynamic parameters, such as Gibb's Free Energy (ΔG), Enthalpy Change (ΔH), Entropy Change (ΔS), Isosteric Heat of Adsorption (ΔH_x), Activation Energy (E_a), Sticking Probability (S^*), Surface Coverage (θ) and Hopping Number (n) were calculated, which are indicators of the possible nature of adsorption. The most suitable adsorption temperature was 40 °C with maximum adsorption capacities of 3.2, 4.5, 4.6 and 4.9 mg/g and the corresponding removal efficiency of 61.81, 81.03, 84.39 and 76.08 %, were obtained for P-Nitrophenol, Naphthalene, Acenaphthene and Pyrene respectively. The ΔH , ΔS , E_a and S^* values were -3694.58, -27102.81, -37004.78 and -138353.27 kJ/mol; -3.1261, -66.5652, -95.7690 and -138353.27 kJ/mol; -3.1261, -66.5652, -95.7690 and -138353.27 kJ/mol; -3.1261, -3.1261407.4775kJ/mol; -3694.58, -27102.81, -37004.78 and -138353.274 gmol $^{-1}$; and 1.4565, 3.0010×10^3 , 1.0061×10^5 and 1.9284×10^5 10²¹ for P-nitrophenol, Naphthalene, Acenaphthene and Pyrene respectively. These values confirm that the adsorption process is favourable and endothermic.

Keywords— Adsorption, Cellulose, Pineapple Crown, Polyaromatic-hydrocarbons, thermodynamics

1. Introduction

The Oil and gas industry's high concentrations of polycyclic aromatics hydrocarbons (PAHs), which are known to be hazardous and possibly carcinogenic to both humans and wildlife make produced water a serious environmental problem. Traditional techniques for eliminating PAHs from Produced water are not suited for broad usage because they are costly and energy-intensive. PAHs are a significant issue due to their intrinsic characteristics which include hydrophobicity, thermostability and heterocyclic aromatic ring topologies which make them resistant and extremely persistent.

A sustainable and economical way to eliminate PAHs from produced water is to make cellulose from pineapple crowns. Cellulose is the most prevalent natural polymer in the world and continues to attract interest because of its high availability, non-toxicity, chemical stability, biodegradability,

biocompatibility, renewability and affordability [9]. It is a partly crystalline, unbranched homopolysaccharide that is insoluble in water and other common solvents due to a robust network of intramolecular and intermolecular hydrogen bonds [6]. Cellulose is therefore a highly desirable material for the removal of toxic substances in generated water.

The most popular edible member of the bromeliaceae family is the pineapple (Ananas comosus) is one of the most significant fruits in the world, its juice is the third most popular around the world, after apple and orange juices [8]. The pineapple crown (upper part of a pineapple fruit) makes up about 10-25% of its total weight [9], its processing generates 3 billion tons of by-products each year and has caused an environmental problem in the agricultural lands. The pineapple crown leaf contains fibres that have a variety of physical characteristics mostly composed of cellulose (79-

⁵ Department of Civil Engineering, Faculty of Engineering, Ladoke Akintola University of Technology, (LAUTECH), Ogbomoso, Nigeria

Vol. 9 Issue 3 March - 2025, Pages: 80-87

83%), Lignin (5-15%), hemicellulose (19%), pectin (1%), waxes (2-3%) and ash (1%) [12]. Natural fibres found in these wastes, particularly pineapple crown leaves are typically recyclable as raw materials for cellulose production [10].

2. MATERIALS AND METHODS

Fresh pineapple crown leaves were washed with distilled water to remove dirt and then dried in a laboratory oven at 100 $^{\circ}\text{C}$ for 3 h. The dried sample derived was then mechanically pulverized and sieved to a particle size of 840-1189 μm (mesh size 20). A total of 300 g of pineapple crown powder was treated with 6.0L of distilled water at 70 $^{\circ}\text{c}$ for 4 h, under strong mechanical stirring (pH 5.0-5.5). Then, the insoluble powder was collected and treated with 5000 mL 10% w/v sodium hydroxide aqueous solution for 24 h at room temperature and then heated for another 30 mins at 80 $^{\circ}\text{c}$ under mechanical stirring. The alkali-treated fibre was washed with deionized water four times until the alkali was completely removed (washed thoroughly until neutrality) and then, it was air dried. The yield of pineapple crown cellulose by the above processing was almost 28% (w/w) [9].

2.1 Batch Adsorption Studies

Samples of the prepared produced water (100 mL) were combined with 1.0 g of the PCC in a 250 mL flask. The flask and its contents were then placed in a rotary shaker and agitated for 60 mins at 180 rpm, with the temperature varying between 40 and 60 °C in 5 °C increments. After agitation, the flasks were removed from the shaker, and the solution was decanted. The supernatant was subsequently centrifuged at 1500 rpm for 20 mins. The concentration of unadsorbed PAHs in the centrifuged sample was measured using a UV-Vis Spectrophotometer at wavelengths 318 nm, 220 nm, 226 nm and 240 nm for P-nitrophenol, Naphthalene, Acenaphthene and Pyrene respectively. The adsorption capacity and percentage removal were then calculated based on Eqns 1 and 2 (Okoye *et al.*, 2018).

$$q_e = \frac{c_o - c_e}{W} \times Volume \tag{1}$$

$$R_e = \frac{c_o - c_e}{c_o} \times 100\% \tag{2}$$

where $C_{\rm o}$ is the initial adsorbate concentration, $C_{\rm e}$ is the equilibrium PAH concentration, V is the volume of solution, and W is the weight of the adsorbent.

2.2 Adsorption Thermodynamics Study

The thermodynamic properties of the selected polyaromatic hydrocarbon adsorption onto the pineapple crown cellulose produced were investigated based on the existing adsorption thermodynamics models. These properties often give insight into the nature (physisorption or chemisorption) and the impact of the temperature-prompted energy of the adsorption process.

2.2.1 Gibb's Free Energy, Enthalpy Change and Entropy Change

The adsorption study examined Gibbs free energy, enthalpy change, and entropy change using Eqns 3-6. The values of ΔH and ΔS were determined from the slope and intercept of the linear plot of ln Kc versus 1/T [1].

$$Kc = \frac{Co}{Ge} \tag{3}$$

$$\Delta G^{\circ} = -RT lnK c \tag{4}$$

$$\Delta G^{\circ} = \Delta H - T \Delta S \tag{5}$$

$$lnKc = \frac{\Delta S}{R} - \frac{\Delta H}{RT} \tag{6}$$

Here, R represents the gas constant (8.314 J/mol·K), T denotes the temperature, and K_c is the equilibrium constant (distribution coefficient). Additionally, C_o refers to the initial concentration of the adsorbate, while C_e indicates the concentration of the adsorbate remaining in the solution (mg/L).

2.2.2 Isosteric heat of adsorption

The isosteric heat of adsorption is defined as the ratio of a minute change in adsorbate enthalpy to a corresponding infinitesimal change in the amount adsorbed while maintaining constant temperature and pressure [13]. This parameter is crucial in characterizing adsorption processes and is typically determined using the Clausius-Clapeyron equation, as shown in Eqn 7.

$$\frac{dlnCe}{dT} = -\frac{\Delta H}{RT^2} \tag{7}$$

By integrating

$$\int dln C_e = \int -\frac{\Delta H}{RT^2} dT \tag{8}$$

Rearrangement of Eqn 8 gave equation (9)

$$lnCe = -\frac{\Delta Hx}{R} \cdot \frac{1}{T} + K \tag{9}$$

where $\Delta H_{\rm X}$ is the isosteric heat of adsorption (kJ mo^{l-1}).

The values of ΔH_X and K were determined from the slope and intercept, respectively from the plot of $\ln C_e$ against 1/T.

2.2.3 Activation Energy and Sorption Probability

Activation energy refers to the minimum energy required for a particular adsorbate-adsorbent interaction, such as a chemical reaction to take place. Sorption probability, a thermodynamic parameter, represents the tendency of an adsorbate to adhere to the surface of an adsorbent permanently. The values of E_a and S^* were determined using Eqns. 10-11 and the plot of $\ln(1-\theta)$ versus 1/T, where the intercept and slope correspond to $\ln S^*$ and E_a/R , respectively.

$$\ln(1-\theta) = \ln S * + \frac{Ea}{RT}$$
 (10)

$$\ln\left(\frac{Co-Ce}{Co}\right) = \frac{Ea}{R} \frac{1}{T} + \ln S * \tag{11}$$

Where; θ is the surface coverage and E_a is the activation energy.

2.2.4 Eyring Equations

The thermodynamic properties (ΔH^{-} and ΔS^{-}) of the Eyring equation from Equations 12 and 13. The values of (ΔH^{-}) and (ΔS^{-}) were calculated from the slope and intercept of the plot of $\ln \frac{K}{T}$ versus $\frac{1}{T}$ [23].

$$ln\frac{K}{T} = \left(\frac{lnKB}{h} + \frac{\Delta S}{R}\right) - \frac{\Delta H}{R} \cdot \frac{1}{T}$$
 (12)

where K_B is the Boltzmann constant (1.3807 \times 10⁻²³ J K⁻¹), h is the Plank constant (6.6261 \times 10⁻³⁴ Js) and R is the universal gas constant (8.314 J mol⁻¹K⁻¹).

2.2.5 Surface Coverage versus the Hopping Number

The hopping number represents the possible number of movements an adsorbate molecule makes while searching for an available site on the adsorbent surface during adsorption [4]. Surface coverage is defined in Eqn 13, while the relationship between θ and n is given in Eqn 14.

$$\theta = \left(1 - \frac{ce}{co}\right) \tag{13}$$

$$n = 1 (1 - \theta)\theta \tag{14}$$

3 RESULTS AND DISCUSSION

3.1 Effect of Temperature on Adsorption

The effect of temperature on the adsorption of Polycyclic Aromatic Hydrocarbons (PAHs) is a crucial factor in determining adsorption efficiency. Based on the bar chart Figure 1, removal efficiency (Re) increases with temperature up to a certain point, indicating an endothermic adsorption process. This suggests that at higher temperatures, PAH molecules gain more kinetic energy, enhancing their diffusion across the adsorbent surface and into available micropores [15]. However, beyond a certain temperature, specifically at 60 °C, a decline in adsorption removal efficiency is observed. This decrease may be attributed to desorption effects, where excessive thermal energy disrupts the adsorbate-adsorbent interactions, leading to reduced retention of PAHs on the adsorbent surface [14].

The most favourable temperature for adsorption appears to be around 50-55 °C, where adsorption efficiency is at its peak. At lower temperatures, such as 40 °C, adsorption is less effective, likely due to insufficient molecular energy to overcome activation barriers for effective surface interaction [17]. Conversely, at excessively high temperatures (60 °C), desorption becomes more prominent, reducing overall adsorption efficiency [16]. These findings align with previous studies, which suggest that adsorption processes involving PAHs often exhibit optimal efficiency within a moderate temperature range before thermal agitation disrupts adsorbate retention [14]. Overall, 50-55 °C is the most favourable temperature range for PAH adsorption, as it provides an optimal balance between enhanced molecular interaction and minimal desorption effects, leading to maximum adsorption efficiency.

The plot of adsorption capacity against temperature in Figure 1, indicates that all adsorbates' adsorption capacity $(q_{\rm e})$ increases with temperature, suggesting an endothermic adsorption process. This trend implies that higher temperatures enhance the interaction between adsorbates and the adsorbent, possibly by increasing surface activity, reducing mass transfer resistance, or improving diffusion into pores. The effect is more pronounced for some compounds, such as pyrene, compared to others like p-nitrophenol, indicating variability in adsorption behavior based on molecular properties.

Table 1 compares the removal efficiencies of various cellulose-based adsorbents for different pollutants at specific temperatures. This suggests that higher temperatures generally enhance adsorption performance. References from previous studies add credibility while this study indicates original research findings on Pineapple crown adsorption.

ISSN: 2643-9085

Vol. 9 Issue 3 March - 2025, Pages: 80-87

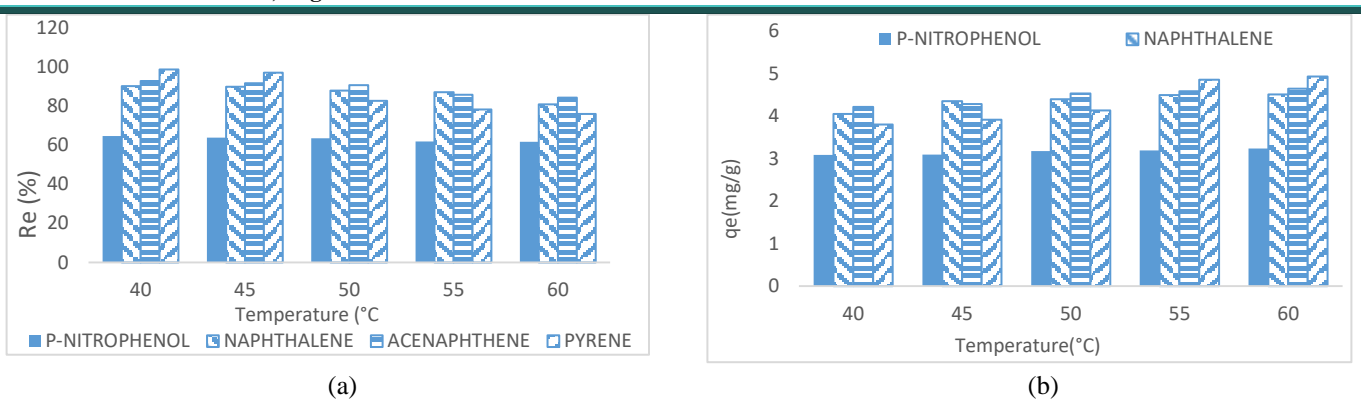


Figure 1: The plot of (a) Removal efficiency against temperature and (b) Adsorption capacity against temperature for the removal of P-Nitrophenol, Naphthalene, Acenaphthene and Pyrene

Cellulose **Pollutant** Temperature Removal References (**K**) Efficiency (%) Cu(I)-Polyaninile composite Orange 16 323 94.99 Kumar et al., 2021 Desert date seed shell-activated carbon Crystal violet 303 50.12 Umar et al., 2020 Activated carbon from apple peel Neutral red 318 87.20 Ali et al., 2023 Pineapple crown P-nitrophenol 313 64.8 This Study Naphthalene 313 90.2 This Study This Study Acenaphthene 313 93.0

313

Pyrene

. Table 1: Comparison of Removal efficiency to other studies

3.2 Thermodynamics Properties

Thermodynamic parameters such as enthalpy change (ΔH), entropy change (ΔS), and Gibbs free energy (ΔG) (Table 2) were determined from the intercept and slope of the plots of ln K_c against 1/T for different temperatures used as shown in Figure 2. Negative values obtained for ΔG at all temperatures confirm the feasibility of the process and the spontaneous nature of the adsorption of the PAHs onto the adsorbent. Higher negative values were obtained at higher temperatures,

suggesting that the adsorption process becomes more spontaneous as temperature increases. The calculated thermodynamic parameters ΔG , ΔH and ΔS for each adsorbate; P-nitrophenol, Naphthalene, Acenaphthene and Pyrene were -3.092 kJ/mol, 2.151 kJ/mol, 16.23 J/mol·K; -3.958 kJ/mol, 4.317 kJ/mol, 25.61 J/mol·K; -4.015 kJ/mol, 4.542 kJ/mol, 26.48 J/mol·K; and -3.928 kJ/mol, 12.768 kJ/mol, 51.66 J/mol·K for P-nitrophenol, Naphthalene, Acenaphthene and Pyrene respectively.

This Study

98.7

Table 2: PAHs uptake dynamic thermodynamics parameters

Adsorbate	Thermodynamics Parameters								
Ausorbate	\mathbb{R}^2	ΔH	ΔS	ΔG (KJ/mol)					
	K	(KJ/mol)	(KJ/gmol K)	313K	318 K	323 K	328 K	333 K	
P-Nitrophenol	0.9446	-3.694600	-0.003126	-2.71611	-2.70048	-2.68485	-2.66922	-2.65359	
Naphthalene	0.8623	-27.10280	-0.066570	-6.26790	-5.93508	-5.60225	-5.26942	-4.93660	
Acenaphthene	0.9447	-37.00480	-0.095769	-7.02908	-6.55024	-6.07139	-5.59255	-5.11370	
Pyrene	0.8719	-138.3533	-0.407478	-10.8128	-8.77543	-6.73804	-4.70065	-2.66326	

The values of ΔG suggest a chemisorption process, as values of ΔG for a physisorption process are generally between -2.77 and -1.27 kJ/mol. The positive values of ΔH confirm the endothermic nature of the adsorption process, while positive ΔS values indicate increased randomness at the solid-liquid interface. Pyrene exhibited the highest increase in adsorption capacity (qe) with temperature, suggesting stronger

adsorbate-adsorbent interactions. The values obtained for ΔH , ΔS , and ΔG align with previous studies, indicating that the adsorption of PAHs onto the adsorbent is a feasible process. The results are consistent with those obtained by Chakraborty *et al.* 2021 [22].

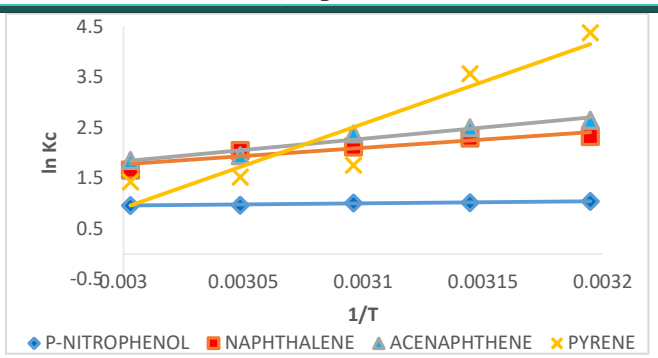


Figure 2: Plot of ln Kc against 1/T

3.2.2 Isosteric Heat of Adsorption

The values of ΔHx were obtained from the slope of a plot of ln Ce versus 1/T, which was found to be linear (Figure 3). The R² values of the isosteres, indicating the goodness of fit, were 0.9446, 0.8623, 0.9447, and 0.8719 for P-Nitrophenol, Naphthalene, Acenaphthene, and Pyrene, respectively. The R² values confirm the strong linear correlation and reliability of the calculated ΔHx values, which are summarized in Table 3.

The magnitude of ΔHx provides insights into the adsorption mechanism, distinguishing between chemical ion exchange and physical adsorption. According to Neimark *et al.* (2017), physical adsorption occurs when ΔHx is below 80 kJ mol⁻¹. In this study, the values of ΔHx were 3.6946, 27.1028, 37.0048, and 138.3532 kJ mol⁻¹ for P-Nitrophenol, Naphthalene, Acenaphthene, and Pyrene, respectively (Figure 3). These results indicate that the adsorption of P-Nitrophenol, Naphthalene, and Acenaphthene onto cellulose was a physical process, whereas Pyrene followed a chemical adsorption mechanism. This suggests surface energetic heterogeneity, where different adsorption sites contribute to varying adsorption strengths based on the adsorbate.

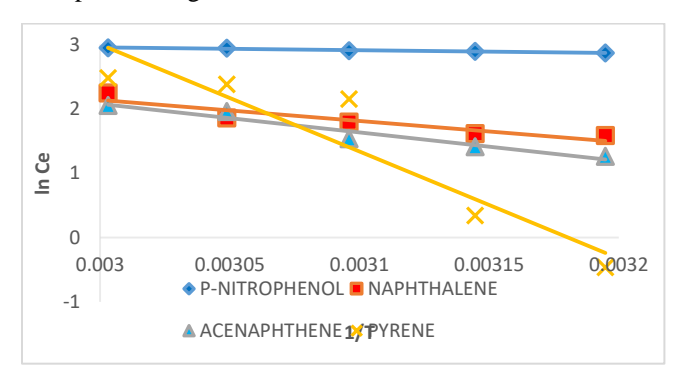


Figure 3: Plot of ln Ce against 1/T

3.2.3 Sticking Probability and Activation Energy

The activation energy (E_a) values calculated from the slope of the plot (Figure 4) were 3694.58 J/mol, 27102.81 J/mol, 37004.78 J/mol, and 138353.27 J/mol for P-Nitrophenol, Naphthalene, Acenaphthene, and Pyrene, respectively. The results shown in Table 3 indicate that the probability of adsorbate sticking to the cellulose surface (S^* values) were 1.46, 3000.10, 100609.30, and 1.93×10^{21} for P-Nitrophenol, Naphthalene, Acenaphthene, and Pyrene, respectively.

The sticking probability should lie within $0 < S^* < 1$, which indicates a physisorption mechanism [24]. However, the high values of S^* , particularly for Naphthalene, Acenaphthene, and Pyrene, suggest a deviation from the expected range. This could imply strong interactions between the PAHs and the cellulose surface or potential limitations in the adsorption model used.

The positive values of E_a confirm that the adsorption process is endothermic, requiring energy for the adsorbate molecules to adhere to the surface. Additionally, the relatively high activation energy values suggest that the adsorption is not diffusion-controlled and may involve stronger interactions between the adsorbate and adsorbent than simple physisorption. Further investigation is needed to confirm the adsorption mechanism and validate the calculated S^* values.

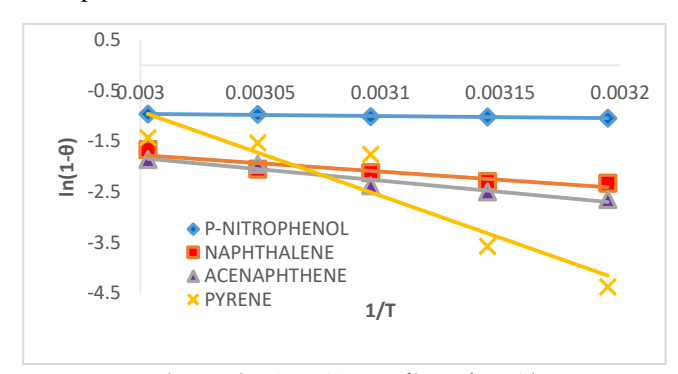


Figure 4: Plot of $ln(1 - \theta)$ against 1/T

3.2.4 Eyring Equation

The thermodynamic parameters for the compounds P-nitrophenol, Naphthalene, Acenaphthene, and Pyrene were determined using the Eyring equation. A plot of $\ln(K/T)$ versus 1/T yielded straight-line equations with slopes and intercepts corresponding to the activation enthalpy (ΔH^-) and entropy (ΔS^-), respectively. The result in Table 4 shows that P-nitrophenol exhibited the lowest activation enthalpy, ΔH^- , -6.38 KJ/mol, indicating a low energy barrier for its reaction. Additionally, its entropy value, ΔS^- , -0.2570 KJ/mol·K was relatively low, suggesting a little or no degree of disorderliness in the transition state. The positive Gibbs free energy, ΔG^- , 70.21 KJ/mol indicates that the process is nonspontaneous under standard conditions.

Vol. 9 Issue 3 March - 2025, Pages: 80-87

Table 3: Isosteric Heat of Adsorption, Sticking Probability and Activation Energy Parameter

Adsorbate	Thermodynamics Parameters							
	\mathbb{R}^2	K	ΔH _x (KJ/mol)	Ea (g mol-1)	S *			
P-Nitrophenol	0.9446	3.6946	4.288	-3694.58	1.4565			
Naphthalene	0.8623	27.1028	11.918	-27102.8086	3000.0973			
Acenaphthene	0.9447	37.0048	15.431	-37004.7826	3000.0973			
Pyrene	0.8719	138.3533	52.923	-138353.274	1.9284×10^{21}			

In contrast, Pyrene demonstrated a much lower activation enthalpy, ΔH^- , -141.04 KJ/mol and negative entropy, ΔS , -0.6614 KJ/mol·K, which suggests a highly ordered transition state. Its positive Gibbs free energy, ΔG , 56.05 KJ/mol reflects a non-spontaneous process under standard conditions. Naphthalene and Acenaphthene exhibited intermediate values, with ΔH^- values of -29.786 KJ/mol and -39.688 KJ/mol, respectively, and negative ΔS . Their Gibbs free energies were 65.71 KJ/mol and 64.51 KJ/mol, respectively.

These findings highlight significant differences in the thermodynamic behavior of the studied compounds. P-Nitrophenol's low activation energy and non-spontaneous nature make it more reactive compared to Pyrene, which requires significantly more energy to overcome its activation barrier. This analysis underscores how thermodynamic parameters derived from the Eyring equation can provide

valuable insights into reaction mechanisms and molecular behavior.

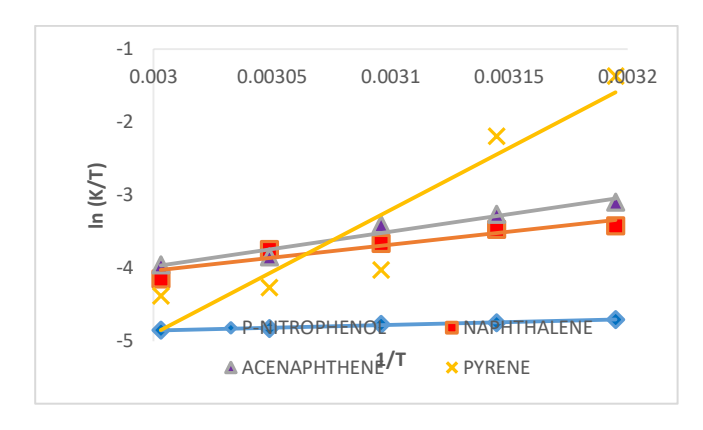


Figure 5: Plot of ln(K/T) against 1/T.

Table 4: PAHs uptake for Eyring equation

Adsorbate		Thermodynamic Parameters							
	\mathbb{R}^2	ΔH ⁻ (KJ/mol)	ΔS ⁻ (KJ/mol)	ΔG- (KJ/mol)					
				313K	318K	323K	328K	333K	
P Nitrophenol	0.9807	-6.378	-0.2570	74.067	75.352	76.637	77.922	79.207	
Naphthalene	0.8829	-29.786	-0.3205	70.518	72.120	73.723	75.325	76.927	
Acenaphthene	0.9514	-39.688	-0.3497	69.753	71.501	73.249	74.997	76.746	
Pyrene	0.8762	-141.039	-0.6614	65.970	69.277	72.584	75.899	79.197	

3.2.5 Surface Coverage vs the Hopping Number

The plot of surface coverage (Θ) versus hopping number (n) indicates the movement of selected PAHs to vacant sites on the adsorbent surface increases with surface coverage. The clustering of P-Nitrophenol data at low 'n' values, along with its high R-squared value (0.9985), suggests that within this observed range of hopping numbers, P-nitrophenol achieves higher surface coverage with fewer hops compared to Naphthalene, Acenaphthene, and Pyrene, potentially indicating faster initial binding. While Naphthalene and Acenaphthene exhibit relatively steep initial increases in

surface coverage, Pyrene demonstrates a more gradual increase. The hopping number describes how fast an adsorption process happens; thus, the smaller the hopping number (n), the faster the sorption process [4].

Vol. 9 Issue 3 March - 2025, Pages: 80-87

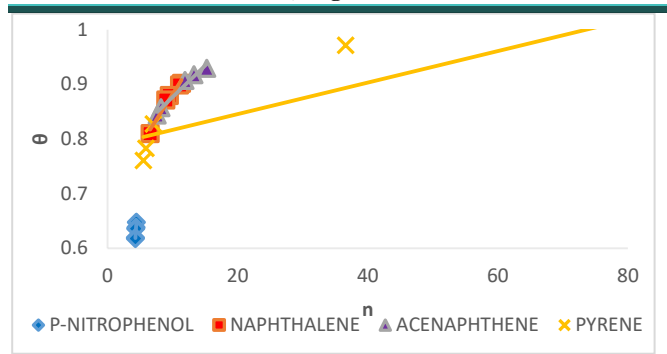


Figure 6: Plot of surface coverage vs hopping number

4 CONCLUSION

This study investigated the removal of a PAH multicomponent mixture from synthesized produced water using pineapple crown cellulose derived from agricultural residues. The adsorption process, involving P-Nitrophenol, Naphthalene, Acenaphthene, and Pyrene, was found to be temperature-dependent, with decreasing PAH concentrations at higher temperatures indicating a low energy requirement for adsorption onto the cellulose. Thermodynamic analysis confirmed that the adsorption process was spontaneous, feasible, and exothermic, exhibiting increased randomness at the interface and an overall affinity for the cellulose adsorbent.

Further insights were gained from the analysis of the surface coverage (O) versus hopping number (n) relationship, revealing differences in the adsorption kinetics among the PAHs. Specifically, P-Nitrophenol demonstrated a rapid increase in surface coverage at low hopping numbers (consistent with its clustered data points and high R2 value of 0.9985 in the Θ vs. n plot), suggesting a faster initial binding to the cellulose. Three trend lines exist for Pyrene: y = $0.0029x + 0.788 (R^2 = 0.781), y = 0.0114x + 0.7632 (R^2 = 0.781)$ 0.9691), and y = 0.0188x + 0.6952 ($R^2 = 0.9603$). Data from the thermodynamic study suggest a relatively high sticking probability for pyrene compared to P-nitrophenol. While the isosteric heat of adsorption values increased with decreasing temperature for all four PAHs. Notably, the isosteric heat of adsorption increased significantly more for pyrene and was the least for P-nitrophenol with temperature. These differences highlight that cellulose-PAH interaction mechanisms and affinity vary based on PAH molecular structure.

Considering the combined evidence of favourable thermodynamic parameters, insights into adsorption kinetics, and the low-cost nature of pineapple crown cellulose, this study supports the potential application of this bio-adsorbent for treating industrial effluents containing PAHs and potentially other pharmaceutical residues. Future research should focus on optimizing cellulose modification strategies to enhance the equilibrium adsorption capacity, particularly

for PAHs like Pyrene, and on evaluating the performance of this material in real-world wastewater matrices.

ACKNOWLEDGEMENT:

I want to acknowledge Bioenvironmental, Water and Engineering Research Group (BWERG) for giving us access to all the resources of the BWERG Laboratory needed to carry out this work.

REFERENCES

- [1] Batool, F., Akbar, J., Iqbal, S., Noreen, S., Syed, N. and Bukhari, A. (2018). Study of Isothermal, Kinetic, and Thermodynamic Parameters for Adsorption of Cadmium: An Overview of Linear and Nonlinear Approach and Error Analysis. *Bioinorganic Chemistry and Applications*. ID 3463724, pp. 1-11
- [2] Ifelebuegu, A.O. and Edet, U.A. (2020). Kinetics, Isotherms, and Thermodynamic Adsorption of Phosphates from Wastewater Using Recycled Brick Waste. *Processes* 8(6); 1-15
- [3] Marczewski, A.W., Seczkowska, M., Deryło-Marczewska, A. and Blachnio, M. (2016). Adsorption equilibrium and kinetics of selected phenoxyacid pesticides on activated carbon: effect of temperature. *Adsorption* 22; 777–790
- [4] Menkiti, M.C., Aneke, M. C., Ejikeme, P. M., Onukwuli, O.D. and Nwasinachi, U.M. (2014). Adsorptive treatment of brewery effluent using activated Chrysophyllum albidium seed shell carbon. SpringerPlus 3, 213 https://doi.org/10.1186/2193-1801-3-21
- [5] Neimark, A. V., Ravikovitch, P. I., Kowalczyk, P. and Cimino, R. T. (2017). Determination of Isosteric Heat of Adsorption by Quenched Solid Density Functional Theory. *American Chemical Society, Langmuir* 33(8); 1769–1779
- [6] Hongjuan Geng, Zaiwu Yuan, Qingrui Fan, Xiaonan Dai, Yue Zhao, Zhaojiang Wang, Menghua Qin (2014). Characterization of Cellulose films regenerated from Acetone/Water Coagulants. *Carbohydrate polymers* 102;438-444
- [7] Sen, T. K. (2014), Evaluation of thermodynamic parameters for adsorption of heavy metals by green adsorbents. *Environmental Chemistry Letters*, 17(4);1-9
- [8] Sen, T. K. (2014). Review on Dye Removal from Its Aqueous Solution into Non-Conventional Adsorbents. Journal of Chemical and Process Engineering, 1(3);1-11
- [9] Upadhyay, A.; Lama, J.P.; Tawata, S. (2013). Utilization of Pineapple Waste: *A Review. J. Food Sci. Technol. Nepal*, 6;10–18

- [10] Prado, K.S.; Spinacé, M.A.S. (2019) Isolation and characterization of cellulose nanocrystals from pineapple crown waste and their potential uses. *Int. J. Biol. Macromol.*, 122; 410–416
- [11] Maraveas, C. (2020). Production of Sustainable and Biodegradable Polymers from Agricultural Waste. *Polymers*, 12(5);1127
- [12] Mahardika, M.; Abral, H.; Kasim, A.; Arief, S.; Asrofi, M(2018). Production of Nanocellulose from Pineapple Leaf Fibers via High-Shear Homogenization and Ultrasonication. *Fibers*, 6;28
- [13] Brinchi, L.; Cotana, F.; Fortunati, E.; Kenny, J.M(2013). Production of nanocrystalline cellulose from lignocellulosic biomass: Technology and applications. *Carbohydr. Polym*;154–169
- [14] Bae, Y.S. and Snurr, R.Q. (2010). Optimal Isosteric Heat of Adsorption for Hydrogen Storage and Delivery using Metal-Organic Frameworks. *Microporous and mesoporous Materials*, 132;300-303
- [15] Huang, W., Zhang, Y., Chen, J., & Wang, L. (2019). Temperature effects on the adsorption of polycyclic aromatic hydrocarbons onto porous adsorbents. *Journal of Environmental Science and Technology*, 53(8);2451-2463
- [16] Lian, F., Song, Z., & Zhu, L. (2022). Adsorption behavior of PAHs on modified adsorbents under varying temperatures. *Chemical Engineering Journal*, 430, 132911
- [17] Wang, S., Wei, Y., & Chen, B. (2018). Influence of temperature on the adsorption kinetics and thermodynamics of PAHs. *Environmental Pollution*, 236; 638-647
- [18] Zhu, X., Li, Q., & Xu, W. (2020). Adsorption mechanisms of PAHs at different temperatures: A

- thermodynamic approach. *Applied Surface Science*, 508;144749
- [19] Umar Bishir Usman, Yunusa, Muhammad B.Ibrahim(2020). Adsorptive Removal of Basic Dyes and Hexavalent Chromium from Synthetic Industrial Adsorbent Effluent: Screening, Kinetic Thermodynamic Studies. I.J Engineering and Manufacturing, 5;54-74
- [20] Ali R.K, Hulya Koyuncu, Ayesenur Turan, Adnan Aldemir(2023). Comparative Research of Isotherm, Kinetic and Thermodynamic Studies for Neutral Red Adsorption by Activated Carbon Prepared from Apple Peel. Water, Air & Soil Pollution 234(6);383
- [21] Prasanna K.O, Tanvir Arfin, Faruq Mohammad, Schin K.K, Murthy Chavali, Aisha N.A, Hmad A.A (2021). Adsorption, Equilibrium Isotherm, and Thermodynamic Studies towards the Removal of Reactive Orange 16 Dye Using Cu(I)-Polyaninile Composite. *Polymers* 13(20):3490
- [22] Sagnik Chakraborty, Anupam Mukherjee, Subhabrata Das, Naga R.Maddela, Saima Iram, Papita Das (2021). Study on Isotherm, Kinetics and Thermodynamics of Adsorption of Crystal Violet Dye by Calcium oxide modified fly ash. *Environ. Eng. Res.* 26(1);190372
- [23] Ebelegi, N.A. (2019) Surface Functionalization of Polyamidoamine Dendrimer for Sorption Studies. Niger Delta University, Bayelsa, Nigeria, 162
- [24] Ebelegi, A., Ayawei, N. and Wankasi, D. (2020). Interpretation of Adsorption Thermodynamics and Kinetics. *Open Journal of Physical Chemistry*, 10, 166-182.